Published in final edited form as:
Hepatology. 2010 April ; 51(4): 1291–1301. doi:10.1002/hep.23471.

Induction of Maf Proteins by Toxic Bile Acid Inhibits Expression of GSH Synthetic Enzymes and Contributes to Cholestatic Liver Injury in Mice

Heping Yang, **Kwangsuk Ko**, **Meng Xia**, **Tony W.H. Li**, **Pilsoo Oh**, **Jiaping Li**, and **Shelly C. Lu**
Division of Gastroenterology and Liver Diseases, USC Research Center for Liver Diseases, Southern California Research Center for Alcoholic Liver and Pancreatic Diseases and Cirrhosis, Keck School of Medicine USC, Los Angeles, California 90033

Abstract

Background and rationale—We previously showed that hepatic expression of GSH synthetic enzymes and GSH levels fell two weeks after bile duct ligation (BDL) in mice. This correlated with a switch in nuclear anti-oxidant response element (ARE) binding activity from nuclear factor-erythroid 2 related factor 2 (Nrf2) to c-Maf/MafG. Our current aims were to examine whether the switch in ARE binding activity from Nrf2 to Mafs is responsible for decreased expression of GSH synthetic enzymes and the outcome of blocking this switch.

Results—HuH-7 cells treated with lithocholic acid (LCA) exhibited a similar pattern of change in GSH synthetic enzyme expression as BDL mice. Nuclear protein levels of Nrf2 fell at 20 hours following LCA treatment while c-Maf and MafG remained persistently induced. These changes translated to ARE nuclear binding activity. Knockdown of c-Maf or MafG individually blunted the LCA-induced fall in Nrf2 ARE binding and increased ARE-dependent promoter activity while combined knockdown was more effective. Knockdown of c-Maf or MafG individually increased the expression of GSH synthetic enzymes and raised GSH levels and combined knockdown exerted additive effect. Ursodeoxycholic acid (UDCA) or S-adenosylmethionine (SAMe) prevented the LCA-induced fall in expression of GSH synthetic enzymes and promoter activity and prevented the increase in MafG and c-Maf levels. In vivo knockdown of the Maf genes protected against fall in GSH enzymes expression, GSH level and liver injury following BDL.

Conclusions—Toxic bile acid induces a switch from Nrf2 to c-Maf/MafG ARE nuclear binding, which leads to decreased expression of GSH synthetic enzymes and GSH levels and contributes to liver injury during BDL. UDCA and SAMe treatment targets this switch.

Keywords

Bile duct ligation; glutamate-cysteine ligase; anti-oxidant response element; ursodeoxycholic acid; S-adenosylmethionine

INTRODUCTION

Cholestatic liver injury continues to be a major cause of chronic liver disease for which treatment options are limited. Ursodeoxycholic acid (UDCA) is the only medication

Contact information. Shelly C. Lu, M.D. Division of Gastrointestinal and Liver Diseases; HMR Bldg., 415, Department of Medicine, Keck School of Medicine USC, 2011 Zonal Ave., Los Angeles, CA, 90033. Phone: (323) 442-2441. Fax: (323) 442-3234. shellylu@usc.edu.

approved for the treatment of primary biliary cirrhosis (PBC) (1) but has no proven efficacy against other chronic cholestatic liver diseases. Even in PBC, only 25 to 30% of the patients have a complete response to UDCA in terms of normalization of biochemical tests and stabilization or improvement of histologic findings in the liver (2). Therefore, more effective treatment against chronic cholestatic liver injury is sorely needed.

Glutathione (GSH) is a tripeptide found in all mammalian cells but is highly concentrated in the liver (3). It is synthesized in the cytosol via two enzymatic steps, the formation of γ-glutamylcysteine from glutamate and cysteine catalyzed by glutamate-cysteine ligase (GCL); and the formation of GSH from γ-glutamylcysteine and glycine catalyzed by GSH synthase (GS) (3). GCL is the rate-limiting enzyme that is made up of two subunits, the catalytic (GCLC) and the modifier (GCLM) subunits (3). GSH protects against oxidative stress, and regulates cell death, inflammatory and fibrotic responses (3). Using bile duct ligation (BDL) as an animal model for chronic cholestatic liver disease, we recently reported that during later stages of BDL in mice, hepatic expression of GSH enzymes decreased markedly along with GSH levels (4). UDCA and S-adenosylmethionine (SAMe), the main cellular methyl donor that is also a precursor for hepatic GSH (5), given alone was able to prevent the fall in enzyme expression and GSH levels but together exerted additional benefit (4). Combined treatment also was more beneficial in preventing BDL-induced liver injury and fibrosis (4). A key finding reported in this earlier work was a fall during later stages of BDL in nuclear factor-erythroid 2 related factor 2 (Nrf2) nuclear binding to the antioxidant response element (ARE), which is present in the promoter region of many genes involved in anti-oxidant defense, including GSH synthetic enzymes (3,4). This coincided with an increase in the expression of several Maf proteins (c-Maf, MafG and MafK) as well as increased c-Maf and MafG nuclear binding to ARE (4). MafG and MafK are small Mafs that have been reported to heterodimerize with Nrf2 to either activate or repress ARE-dependent genes (6,7). Small Mafs lack transcriptional activation domain and can form homodimers to repress ARE-mediated gene expression (8). In addition, large Maf protein such as c-Maf can bind to ARE as homodimers and heterodimers with small Mafs to repress ARE-mediated gene expression (9). Given these known effects of small Mafs and c-Maf, we speculated that the induction in Mafs and displacement of Nrf2 from nuclear binding to ARE during cholestasis might have caused the fall in the expression of GSH synthetic enzymes. Since GSH plays a key role in anti-oxidant defense, we also speculated this could have further contributed to liver injury. The aims of the current work were to establish a cause-and-effect relationship between displacement of Nrf2 by Mafs in nuclear ARE binding and the fall in expression of GSH synthetic enzymes, and to examine the functional outcome of blocking induction in Mafs on expression of GSH synthetic enzymes and BDL-induced liver injury.

MATERIALS AND METHODS

Materials

UDCA was obtained from Sigma-Aldrich (St. Louis, MO). S-adenosylmethionine (SAMe) in the form of disulfate p-toluenesulfonate dried powder was generously provided by Gnosis SRL (Cairate, Italy). α-^{32}P-dCTP and γ-^{32}P ATP (3,000 Ci/mmol) was purchased from PerkinElmer (Boston, MA). All other reagents were of analytical grade and obtained from commercial sources.

Cell culture

HuH-7, 293T cell lines and isolated mouse hepatocytes were obtained from the Cell Culture Core of the USC Research Center for Liver Diseases. Cultures were maintained in DMEM medium supplemented with 10% fetal calf serum, 2 mM L-glutamine, and 1% penicillin-

streptomycin. Mouse hepatocytes were isolated from BDL mice at indicated days post surgery, centrifuged and purified through Percoll as described (10).

Lithocholic acid (LCA), UDCA, SAMe and siRNA treatments in HuH-7 cells

HuH-7 cells were treated with LCA (100 μM) for up to 24 hours and processed for gene and protein expression analysis, GSH level and promoter activity measurements as described below. In other experiments, HuH-7 cells were treated with LCA, UDCA, SAMe (all 100 μM), UDCA plus SAMe, or combination of LCA with UDCA and/or SAMe for 20 hours and processed for gene expression analysis and promoter activity measurement as described below.

Double-stranded MafG, c-Maf and scrambled siRNA (MafG siRNA cat# sc-38099, c-Maf siRNA cat# sc-38111) were purchased from Santa Cruz Biotechnology (Santa Cruz, CA). HuH-7 cells were transfected with MafG, c-Maf, MafG plus c-Maf or scrambled siRNA (10 nM per 1×10^5 cells) using Lipofectamine™ RNAiMAX Transfection Reagent (Invitrogen) in 6 well plates at 30% confluency for up to 72 hours and processed for Western blot analysis, promoter activity measurement or GSH level determination as described below. In other experiments, HuH-7 cells transfected with above siRNA for 24 hours were subsequently treated with LCA (100 μM) for another 20 hours and processed for Western blot analyses and electrophoretic mobility shift assay (EMSA) and supershift assay for ARE nuclear binding as we described (4).

BDL in mice

Three-month old male C57/B6 mice were fed chow ad libitum, and housed at constant temperature (22°C) with alternating 12 hours of light and darkness. The mouse procedure protocols, use and the care of the animals were reviewed and approved by the Institutional Animal Care and Use Committee at the University of Southern California. BDL and sham surgery were performed as we described (4). Mice were sacrificed on indicated days post surgery and livers were harvested for studies described below.

Necrosis, apoptosis, and fibrosis determination in liver specimens

Formalin-fixed liver tissues embedded in paraffin were cut and stained with hematoxylin and eosin (H&E) and the percentage of necrosis was estimated by counting the number of microscopic fields with necrosis compared to the entire section in 15 different sections at 100× magnification. Apoptosis was determined by staining with Terminal deoxynucleotidyl transferase (TdT)-mediated dUTP-digoxigenin nick-end labeling (TUNEL) according to the manufacturer's (*In situ* cell death detection kit, Roche) suggested protocol. Five random fields containing an average of 250 nuclei were counted for each TUNEL-stained tissue sample. The apoptotic index (percentage of apoptotic nuclei) of hepatocytes was calculated as (apoptotic nuclei/total nuclei) ×100%. Samples from at least three mice per treatment condition were scored. Fibrosis was determined by staining with 0.1% Sirius red (Sigma, St. Louis, MO) and quantified using a computer-assisted image analysis system (MetaMorph imaging system; Universal Imaging Corporation, Downingtown, PA) and expressed as stained area per total examined area.

RNA isolation and gene expression analysis

Total RNA was isolated by the TRIzol reagent (Invitrogen) from liver tissues. Northern blot analysis, autoradiography and densitometry were done as previous described (4). The mouse specific cDNA probes for Northern blot include: GCLC - nucleotides 120–610 (NM_010295), GCLM - nucleotides 411–905 (NM_008129), and GS - nucleotides 181–695 (NM_008131). Specific GCLC, GCLM, GS and β-actin probes were labeled with

[^{32}P]dCTP using a random-primer kit (RediPrime DNA Labeling System; Amersham Pharmacia Biotech) as described (4). Results of Northern blot analysis were normalized to β-actin.

Western blot analysis

Liver tissues from BDL mice and HuH-7 cells after various treatments were subjected to Western blot analysis as described (4). Nuclear protein was isolated as described (4). Equal amounts of total protein extracts (15 μg/well) were resolved on 12.5% SDS–polyacrylamide gels. Membranes were probed with antibodies to GCLC, GCLM (Novus Biologicals, Littleton, CO), GS, Nrf2, c-Maf, (Santa Cruz Biotechnology, Santa Cruz, CA), MafK, and MafG (R&D Systems, Minneapolis, MN). To ensure equal loading, membranes were stripped and re-probed with anti-actin or anti-Histone 3 antibodies (Santa Cruz Biotechnology, Santa Cruz, CA) for total versus nuclear protein levels, respectively. Blots were developed by enhanced chemiluminescence (Millipore Corporation, Billerica, MA).

Electrophoretic mobility shift assay and supershift assay

EMSAs were done as described previously (11). The probe was ^{32}P-end-labeled double-stranded ARE DNA fragment (CTGGAAGACAATGACTAAGCAGAAA), corresponding to −315 to −339 bp relative to the translation start codon of mouse GCLM (NM_008129), with the core ARE sequence underlined. Supershift assays confirmed the identity of the binding proteins using antibodies to Nrf1, Nrf2, c-Maf, or MafG (Santa Cruz Biotechnology Inc., Santa Cruz, CA or R&D Systems, Minneapolis, MN) as we described (11).

Chromatin immunoprecipitation (ChIP) assay

To verify changes in protein binding to the ARE4 of the human GCLC and the key ARE of the human GCLM promoters in an endogenous chromatin configuration, ChIP assay was carried out following the ChIP assay kit protocol provided by Upstate (Waltham, MA). HuH-7 cells were treated with LCA (100 μM for 20 hrs) or vehicle control and processed for ChIP assay as we described (11). Antibodies used for immunoprecipitation were anti-Nrf2, Nrf1, c-Maf, MafG and Histone 3 antibodies (Santa Cruz Biotechnology). PCRs of the human GCLC promoter region across ARE4 (GCGCTGAGTCAC, −3708/−3697bp relative to ATG start site) (GenBank® accession no. AY382195) used forward primer 5'-TCCTTGGAGGCCCGAAACCCATC-3’ (bp −3853 to −3831) and reverse primer 5'-ACCGCCTCCCCGTGACTCAGC-3' (bp −3706 to −3686). PCRs of the human GCLM promoter region across the ARE (TGCTTAGTCAT, −302/−292bp relative to the ATG start site) (GenBank® accession no. AY382196) used forward primer 5'-CGCGGGATGAGTAACGGTTAC-3’ (bp −348 to −328) and reverse primer 5'-CGGGAAAGGAAGGCACCGGTG-3' (bp −212 to −192). All PCR products were run on 8% acrylamide gels and stained with ethidium bromide for 15–30 min.

Promoter constructs and transient transfection assays

Human GCLM (−712/+3-LUC, where LUC stands for luciferase) promoter construct containing functional ARE was kindly provided by Benassi and colleagues (12). To clone the promoter region of the human GCLC gene, a reverse primer (5’-CAGCCTAATCTGGGAAATGAAGTTATTC -3’) corresponding to +427 to +455 (numbered according to the translational start site) of the human GCLC cDNA (GenBank® accession no. NM_001498) and a forward primer (5’-AGCAGCAGCAGCCCAGAGGTCAG -3’) corresponding to −3802 to −3779 (numbered according to the ATG start site) of our reported human GCLC 5’-flank region (GenBank® accession no. AY382195) was used for PCR amplification (Advantage 2 PCR Enzyme system; BD Biosciences Clontech, Palo Alto, CA, U.S.A.) of a human genomic DNA

(Genome Walker, Clontech). A positive clone was identified and sequenced using the ABI Prism dRhodamine Terminator Cycle Sequencer performed by the Microchemical Core Facility (Norris Comprehensive Cancer Center, Keck School of Medicine). This 3.8 kb 5´-flanking region of the human GCLC was cloned into pGL3-basic vector creating the recombinant plasmid −3802/+455 GCLC-LUC. In addition, a wild type (HindIII linker (ATCGAAGCTT)+(AAG**CGCTGAGTCAC**GGG)2+BglII linker (AGATCTAGCT) and a mutant ARE-4 (HindIII linker+(AAG**CGCTATGTCAC**GGG)2+BglII linker) construct based on the human GCLC promoter sequence was created by DNA Oligonucleotide Synthesis (USC DNA Core) and subcloned into pLuc-MCS vector (Stratagene, La Jolla, CA - cat#219087). HuH-7 cells were transfected with these constructs for 3 hours and treated with 100 μM of LCA, UDCA, SAMe, UDCA plus SAMe either alone or together for 20 hours. Control cells were transfected in similar fashion and treated with vehicle. In other experiments, HuH-7 cells were treated with siRNA against c-Maf, MafG, c-Maf and MafG or scrambled siRNA for 24 hours and then transfected with wild type or mutant ARE-promoter constructs for 8 hours. Luciferase activity was determined as we described and reported as fold of vector control (13).

Knockdown of Mafs in vivo during BDL

The shRNA pre-made lentivirus MafG (cat# VGM5520-98740361), c-Maf (cat# VGM5520-98971408), empty lentivirus (cat# RHS4349) vectors, packaging plasmid, Trans-Lentiviral pGIPZ Packaging System (Cat#TLP4614) and envelope plasmid were purchased from Open Biosystems (Rockford, IL) and viral harvesting was done as described in protocol. A total of 1×10^5 HuH-7 cells were infected at a multiplicity of 20 plaque-forming units/cell for 24 hours. One to 2×10^9 transducing units (1×10^9 for each siRNA, final volume 0.1mL) were injected into the spleen of BDL and sham operated mice immediately after the BDL was performed under the same anesthesia. Second and 3rd injections on days 6 and 10 were performed through the tail vein. Hepatocytes were isolated on day 3, 7, 10 and 14 to assess transduction efficiency using green fluorescent protein (GFP), which is included in the lentivirus vector.

GSH levels

GSH levels in liver tissues and HuH-7 cells were measured as described (13,14).

Serum alkaline phosphatase (ALP), bilirubin and Alanine Transaminase (ALT) levels

Serum ALP, bilirubin (Thermo Electron Corp., Waltham, MA) and ALT (RAICHEM, San Marcos, CA) levels were measured following manufacturers' instruction.

Statistical Analysis

Data are given as mean ± standard error of the mean (SEM). Statistical analysis was performed using analysis of variance followed by Fisher's test for multiple comparisons. For changes in mRNA and protein levels, ratios of genes or proteins to housekeeping genes or proteins densitometric values were compared. Significance was defined by $p<0.05$.

RESULTS

Changes in the expression of GSH synthetic enzymes following LCA, UDCA and SAMe treatment in HuH-7 cells

To facilitate investigation of molecular mechanisms, we used LCA (100 μM) treated HuH-7 cells as an in vitro model (15). Figure 1 shows that LCA treatment in HuH-7 cells induced an early increase in the mRNA (Fig. 1A) and protein (Fig. 1B) levels of GCLC, GCLM and GS followed by a fall to below baseline levels by 20 hours after treatment. Treatment with

LCA for 20 hours did not induce apoptosis in HuH-7 cells but longer treatment did (15). Consistent with these changes, cell GSH levels increased early on but fell by 20 hours after LCA treatment (control cell GSH = 20.0±0.8, LCA for 8 hours = 34.7±0.9, LCA for 20 hours = 12.4±0.6 nmol/mg protein, results are mean±SE from 4 determinations per condition, $p<0.05$ between both LCA treatment time points and control). We previously showed that UDCA or SAMe treatment during BDL prevented the fall in expression of GSH synthetic enzymes with the combination exerting better effect than either alone (4). Figure 1C shows that this is also true in HuH-7 cells so that either agent alone protected partially against the fall but combined treatment completely prevented the fall in expression of GSH synthetic enzymes.

Expression of Nrf2, Maf proteins, ARE nuclear binding and GCL promoter activities following LCA, UDCA and SAMe treatment in HuH-7 cells

The fall in expression of GSH synthetic enzymes during BDL correlated with an induction in Maf proteins (specifically MafG, c-Maf and MafK) and displacement of Nrf2 nuclear binding to ARE by Maf proteins (4). Figure 2 shows that LCA treatment of HuH-7 cells also led to a persistent increase in the nuclear levels of MafG and c-Maf, but MafK levels were unchanged and Nrf2 level fell by 20 hours (Fig. 2A). These changes translated to ARE nuclear binding with a fall in Nrf2 (and Nrf1) and increase in MafG and c-Maf binding following LCA treatment for 20 hours on EMSA with supershift (Fig. 2B) and in the endogenous chromatin configuration as demonstrated with ChIP assays (Fig. 2C). In the BDL model, combined UDCA and SAMe treatment raised nuclear Nrf2 levels and prevented the induction in Maf proteins (4). The same is also true in HuH-7 cells where combined UDCA and SAMe treatment prevented LCA-induced decrease in Nrf2 and increase in MafG and c-Maf levels (Fig. 3A). To see if these changes affect the promoter activity of GCLC and GCLM, HuH-7 cells were transiently transfected with either human GCLC or GCLM promoter constructs that contain functional ARE elements (12). LCA treatment for 20 hours inhibited the promoter activity of GCLC and GCLM, while UDCA or SAMe alone blunted this inhibition and combined UDCA with SAMe completely protected against the inhibition (Fig. 3B and C).

Effect of Maf knockdown on ARE nuclear binding activity and ARE-dependent promoter activity

We next investigated the effect of Maf knockdown on ARE nuclear binding activity. MafG or c-Maf knockdown reduced basal protein levels by 50% (c-Maf) to 60% (MafG) and completely prevented LCA-mediated induction (Fig. 4A and B). These changes translated to an increase in Nrf2 binding to ARE (Fig. 4C and D). However, knockdown of both MafG and c-Maf (double siRNA) exerted much better effect than either Maf siRNA alone in enhancing Nrf2 binding to ARE (Fig. 5A). These changes correlated with ARE-dependent promoter activity so that knockdown of either MafG or c-Maf raised ARE-dependent promoter activity slightly but combined knockdown was more effective. If the ARE binding site was mutated, knockdown of these Maf proteins exerted no influence on promoter activity (Fig. 5B).

Effect of Maf knockdown on expression of GSH synthetic enzymes and GSH levels

Knockdown of either MafG or c-Maf exerted a time-dependent increase in the mRNA (Fig. 6A and B) and protein (Fig. 6C and D) levels of GCLC, GCLM and GS with maximal increase observed at 48 hours (150 to 200% of baseline for all in mRNA and protein levels). Combined knockdown of both MafG and c-Maf raised GCLC, GCLM and GS protein levels in additive fashion (280 to 320% of SC) as compared to either knockdown alone (140 to 160% of SC) (Fig. 6E). As expected, cell GSH levels increased with knockdown of MafG or c-Maf and were highest with combined knockdown of both (Fig. 6F).

Effects of Maf knockdown during BDL

To see if Maf induction is responsible for the fall in expression of GSH synthetic enzymes during BDL and whether this contributes to liver injury, we used the lentiviral gene delivery method to prevent induction of MafG or c-Maf or both during BDL. Pilot experiment was performed to optimize efficiency of transduction and Fig. 7A shows that single injection was ineffective in maintaining knockdown when examined 14 days later. Instead, injection had to be repeated on day 6 and 10 in order to maintain high transduction efficiency on day 14 (Fig. 7A). Knockdown of either Maf proteins protected slightly (25% lower) against necrosis and apoptosis but combined knockdown reduced both by 55% (see Table I for quantitation). Combined knockdown also protected against fibrosis by 56%. These changes are consistent with biochemical parameters of liver injury, which show much lower ALT, bilirubin and ALP levels when either of the Maf genes was knocked down and a tendency for even lower bilirubin and ALP levels with combined knockdown (Table I).

Effect of Maf knockdown on expression of Mafs and GSH synthetic enzymes, ARE nuclear binding activity and GSH levels during BDL

Fig. 8 confirms that MafG and c-Maf knockdown effectively prevented induction of these proteins (Fig. 8A) during BDL and prevented against the fall in GSH synthetic enzymes (Fig. 8B). Actually, knockdown of MafG or c-Maf resulted in higher protein levels of GSH synthetic enzymes (70 to 100% higher) and Nrf2 (50 to 60% higher), even after BDL. Knockdown of MafG or c-Maf also increased Nrf2 nuclear binding to ARE (Fig. 8C), and protected against the fall in hepatic GSH levels (Fig. 8D). Combined knockdown was more effective in protecting expression of GSH synthetic enzymes, increasing Nrf2 nuclear binding to ARE and GSH levels.

DISCUSSION

Liver plays a central role in interorgan homeostasis of GSH and has the highest GSH content of all organs (16). The expression of hepatic GSH synthetic enzymes is reduced in many conditions such as diabetes mellitus (17,18), alcoholic hepatitis (19), during aging (20), endotoxemia (14) and chronic cholestasis (4). In addition to antioxidant defense, recent reports show that GSH also modulates cell death, inflammatory and fibrogenic responses (reviewed in 3). Our recent report showing expression of GSH synthetic enzymes falls markedly during prolonged cholestasis (4) raises the possibility that this can further contribute to liver injury and elucidating the molecular mechanism(s) of this fall might uncover new strategies to treat cholestatic liver injury. The focus of the current work was to establish the molecular mechanism for the fall in expression of GSH synthetic enzymes during cholestasis.

Our earlier work provided an important clue with regards to the mechanism, namely a fall in Nrf2 nuclear binding to ARE during prolonged cholestasis (4). ARE is an important *cis*-acting regulatory element found in the 5'-regulatory region of almost all of the enzymes involved in phase II metabolism of xenobiotics (7). These phase 2 enzymes include GCL, quinone reductase, glutathione S-transferase, epoxide hydrolase, and sulfotransferase and they play important roles in protecting cells against oxidative stress and toxins (6). The transcription factor most well characterized to activate ARE is Nrf2 (6). Nrf2 and a related family member Nrf1 are members of the cap 'n' collar-basic leucine zipper proteins (CNC-bZIP) and both can *trans*-activate ARE (6,21). Nrf2 is kept in the cytosol by Keap1 under non-stressful conditions and undergoes proteosomal degradation (22). Upon recognition of signals imparted by oxidative and electrophilic molecules, Nrf2 is released from Keap1, escapes proteosomal degradation and translocates to the nucleus to induce genes involved in defense and survival (22). In contrast, Keap1 does not control Nrf1's activity (23). Instead,

Nrf1 is primarily localized to the membrane of the endoplasmic reticulum and is released and translocates to the nucleus during endoplasmic reticulum stress (23).

Nrf2 is known to form heterodimers with small Maf (MafG, MafK and MafF) and Jun (c-Jun, Jun-D, and Jun-B) proteins to bind to ARE (6). However, the effect of its binding partner has been controversial, as both activation and repression have been reported with heterodimers of Nrf2 and small Maf proteins (6,7). The small Mafs can form homodimers to repress ARE-mediated gene expression (6). In addition, c-Maf, a large Maf protein can also form heterodimers with small Mafs (but not Nrf2) to repress ARE-mediated gene expression (9). The small Mafs are under complex control, both transcriptional and post-translational and are responsive in particular to stressful stimuli (24). The large Mafs are major regulators of tissue-specific gene expression and cellular differentiation in mammals (24). During prolonged BDL we reported persistent increase in nuclear levels of MafG, MafK and c-Maf and displacement of Nrf2 from ARE nuclear binding (4). These findings supported a role for these changes in causing decreased expression of GSH synthetic enzymes. Our current work provided proof that this is indeed the case.

We used the in vitro model of LCA-treated HuH-7 cells because this model is derived from human and recapitulated many changes observed during BDL in mice (15). This can allow dissection of the molecular mechanisms more easily and reinforce the significance of the findings since they are human in origin. Indeed, we observed very similar pattern of change (early increase followed by a fall) in expression of GSH synthetic enzymes in LCA-treated HuH-7 cells as compared to BDL in mice. UDCA and SAMe treatment protected against this fall and the combination worked better than single agent alone, as we observed during BDL (4). Like in BDL, we noted persistent increase in nuclear levels of MafG and c-Maf after LCA treatment in HuH-7 cells but unlike BDL, MafK levels were unchanged and Nrf2 levels fell. This difference may reflect not only in vitro versus in vivo models, but also species difference. Importantly, LCA treatment for 20 hours also led to a displacement in ARE nuclear binding from Nrf2 to MafG and c-Maf. UDCA and SAMe treatment prevented the LCA-mediated increase in Maf proteins and the decrease in Nrf2. Similar changes were also observed with the human GCLC and GCLM promoter activity. The proof that MafG and c-Maf induction led to the fall in GSH synthetic enzymes is the fact that Nrf2 nuclear binding activity to ARE increased when MafG or c-Maf expression was reduced, and increased even further when both were reduced. This led to similar changes in the ARE-dependent promoter activity, expression of GSH synthetic enzymes and importantly, cell GSH levels. Finally, when induction in Mafs was prevented during BDL by RNAi, it prevented the fall in expression of the GSH synthetic enzymes, increased Nrf2 nuclear binding activity to ARE, GSH levels, and greatly ameliorated biochemical parameters of liver injury, as well as histologic evidence of necrosis, apoptosis and fibrosis. Taken together, this shows that increased expression of Maf proteins such as MafG and c-Maf that occur during cholestasis can inhibit ARE-mediated gene expression by displacing Nrf2 and contribute to liver injury. These results are consistent with a previous report that in an immortalized human bronchial epithelial cell line HBE1 curcumin-induced increase in GCL expression was correlated with a fall in Mafs and increase in Nrf2 binding to ARE (25). To our knowledge, this is the first demonstration of increased Maf protein expression being linked to liver injury. Given the fact that ARE-mediated genes include many enzymes that participate in antioxidant defense, targets besides GSH synthetic enzymes are impacted. Uncovering the molecular signaling pathways that lead to increased nuclear MafG and c-Maf levels during cholestasis will be a future goal as blocking this pathway is likely to result in new therapeutic approaches to treat cholestatic liver injury.

Although our findings support a key role for Nrf2 in protecting the liver against cholestatic liver injury, there are conflicting data on the effect of BDL in Nrf2 knockout (KO) mice.

Aleksunes et al examined BDL in Nrf2 KO mice and found no worsening of injury on day 3 after BDL (26). Later time points were not examined. In contrast, Xu et al found Nrf2 KO mice developed much more liver injury, inflammation and fibrosis following acute and chronic treatment with CCl_4 (up to 45 days). They mentioned that some Nrf2 KO mice had much worse injury following BDL but stated the results were variable (27). Thus, the results from the Nrf2 KO mice are inconclusive. However, with KO mice there can be compensatory mechanisms that develop with time to further confuse this issue.

In conclusion, we have provided conclusive evidence that toxic bile acid can increase the nuclear levels of MafG and c-Maf to displace Nrf2 from binding to ARE. This results in suppression of ARE-mediated genes such as the GSH synthetic enzymes. Blocking the increase in MafG and c-Maf levels prevented the fall in expression of GSH synthetic enzymes and GSH levels during BDL in mice and LCA-treated HuH-7 cells. Most importantly, blocking MafG and c-Maf induction during BDL also ameliorated against liver injury and fibrosis.

List of abbreviations (in alphabetical order)

ALP	alkaline phosphatase
ALT	alanine transaminase
ARE	antioxidant response element
BDL	bile duct ligation
ChIP	chromatin immunoprecipitation
CNC	cap ‘n’ collar
EMSA	electrophoretic mobility shift assay
GCL	glutamate-cysteine ligase
GCLC	GCL-catalytic subunit
GCLM	GCL-modifier subunit
GFP	green fluorescent protein
GSH	reduced glutathione
GS	GSH synthase
H&E	hematoxylin and eosin
KO	knockout
Nrf1	nuclear factor-erythroid 2 related factor 1
Nrf2	nuclear factor-erythroid 2 related factor 2
PBC	primary biliary cirrhosis
SAMe	S-adenosylmethionine
SC	scrambled
TUNEL	terminal deoxynucleotidyl transferase (TdT)-mediated dUTP-digoxigenin nick-end labeling
UDCA	ursodeoxycholic acid

Acknowledgments

Financial support.

This work was supported by NIH grants DK45334 and AT1576 (to S. C. Lu and H. Yang). HuH-7, 293T cells and isolated mouse hepatocytes were provided by the Cell Culture Core and pathological sections & staining were done by the Imaging Core of the USC Research Center for Liver Diseases (P30DK48522).

REFERENCES

1. Kumar D, Tandon RK. Use of ursodeoxycholic acid in liver disease. J. Gastro and Hepatol. 2001; 16:3–14.
2. Silveira MG, Lindor KD. Treatment of primary biliary cirrhosis: Therapy with choleretic and immunosuppressive agents. Clin Liver Dis. 2008; 12:425–443. [PubMed: 18456189]
3. Lu SC. Regulation of glutathione synthesis. Mol Asp Med. 2009; 30:42–59.
4. Yang HP, Ramani K, Xia M, Ko KS, Li TWH, Oh P, et al. Dysregulation of glutathione synthesis during cholestasis in mice: molecular mechanisms and therapeutic implications. Hepatology. 2009; 49:1982–1991. [PubMed: 19399914]
5. Lu SC. Molecule in focus: S-adenosylmethionine. Int J Biochem Cell Biol. 2000; 32:391–395. [PubMed: 10762064]
6. Jaiswal AK. Nrf2 signaling in coordinated activation of antioxidant gene expression. Free Radical Biol. & Med. 2004; 36:1199–1207. [PubMed: 15110384]
7. Nguyen T, Huang HC, Pickett CB. Transcriptional regulation of the antioxidant response element. J. Biol. Chem. 2000; 275:15466–15473. [PubMed: 10747902]
8. Dhakshinamoorthy S, Jaiswal AK. Small Maf (MafG and MafK) proteins negatively regulate antioxidant response element-mediated expression and antioxidant induction of the NAD(P)H:Quinone oxidoreductase 1 gene. J. Biol. Chem. 2000; 275:40134–40141. [PubMed: 11013233]
9. Dhakshinamoorthy S, Jaiswal AK. C-Maf negatively regulates ARE-mediated detoxifying enzyme genes expression and anti-oxidant induction. Oncogene. 2002; 21:5301–5312. [PubMed: 12149651]
10. Kreamer BL, Staecker JL, Sawada N, Sattler GL, Hsia MT, Pitot HC. Use of a low-speed, iso-density percoll centrifugation method to increase the viability of isolated rat hepatocyte preparations. In Vitro Cell Dev Biol. 1986; 22:201–211. [PubMed: 2871008]
11. Yang HP, Magilnick N, Ou XP, Lu SC. Tumor necrosis alpha induces coordinated activation of rat GSH synthetic enzymes via NFκB and AP-1. Biochem. J. 2005; 391:399–408. [PubMed: 16011481]
12. Benassi B, Fanciulli M, Fiorentino F, Porrello A, Chiorino G, Loda M, et al. c-Myc phosphorylation is required for cellular response to oxidative stress. Mol. Cell. 2006; 21:509–519. [PubMed: 16483932]
13. Yang HP, Magilnick N, Lee C, Kalmaz D, Ou XP, Chan JY, et al. Nrf1 and Nrf2 regulate rat glutamate-cysteine ligase catalytic subunit transcription indirectly via AP-1 and NFκB. Mol. Cell Biol. 2005; 25:5933–5946. [PubMed: 15988009]
14. Ko KS, Yang HP, Noureddin M, Iglesia-Ara A, Xia M, Wagner C, et al. Changes in S-adenosylmethionine and glutathione homeostasis during endotoxemia in mice. Lab Invest. 2008; 88:1121–1129. [PubMed: 18695670]
15. Yang HP, Li TWH, Ko KS, Xia M, Lu SC. Switch from Mnt-Max to Myc-Max induces p53 and cycli D1 expression and apoptosis during cholestasis in mice and human hepatocytes. Hepatology. 2009; 49:860–870. [PubMed: 19086036]
16. Ookhtens M, Kaplowitz N. Role of the liver in interorgan homeostasis of glutathione and cyst(e)ine. Sem. Liv. Dis. 1998; 18:313–329.
17. Lu SC, Ge J, Kuhlenkamp J, Kaplowitz N. Insulin and glucocorticoid dependence of hepatic γ-glutamylcysteine synthetase and GSH synthesis in the rat: Studies in cultured hepatocytes and in vivo. J. Clin. Invest. 1992; 90:524–532. [PubMed: 1353765]
18. Cai J, Sun WM, Lu SC. Hormonal and cell density regulation of hepatic γ-glutamylcysteine synthetase gene expression. Molecular Pharmacol. 1995; 48:212–218. 1995.

19. Lee TD, Sadda ME, Mendler MH, Bottiglieri T, Kanel G, Mato JM, et al. Abnormal hepatic methionine and GSH metabolism in patients with alcoholic hepatitis. Alcoholism: Clin. Exp. Res. 2004; 28:173–181.

20. Wang H, Liu H, Liu RM. Gender difference in glutathione metabolism during aging in mice. Exp. Gerontology. 2003; 38:507–517.

21. Kwong M, Kan YW, Chan JY. The CNC basic leucine zipper factor, Nrf1, is essential for cell survival in response to oxidative stress-inducing agents. J. Biol. Chem. 1999; 274:37491–37498. [PubMed: 10601325]

22. Kensler TW, Wakabayashi N, Biswal S. Cell survival responses to environmental stresses via the Keap1-Nrf2-ARE pathway. Annu. Rev. Pharmacol, Toxicol. 2007; 47:89–116. [PubMed: 16968214]

23. Wang W, Chan JY. Nrf1 is targeted to the endoplasmic reticulum membrane by an N-terminal transmembrane domain. J. Biol. Chem. 2006; 281:19676–19687. [PubMed: 16687406]

24. Blank V. Small Maf proteins in mammalian gene control: mere dimerization partners or dynamic transcriptional regulators? J. Mol. Biol. 2008; 376:913–925. [PubMed: 18201722]

25. Dickinson DA, Iles KE, Zhang H, Blank V, Forman HJ. Curcumin alters EpRE and AP-1 binding complexes and elevates glutamate-cysteine ligase gene expression. FASEB J. 2003; 17:473–475. [PubMed: 12514113]

26. Aleksunes LM, Slitt AL, Maher JM, Dieter MZ, Knight TR, et al. Nuclear factor-E2-related factor 2 expression in liver is critical for induction of NAD(P)H:quinone oxidoreductase 1 during cholestasis. Cell Stress & Chaperones. 2006; 11:356–363. [PubMed: 17278884]

27. Xu W, Hellerbrand C, Köhler UA, Bugnon P, Kan YW, Werner S, et al. The Nrf2 transcription factor protects from toxin-induced liver injury and fibrosis. Lab. Invest. 2008; 88:1068–1078.

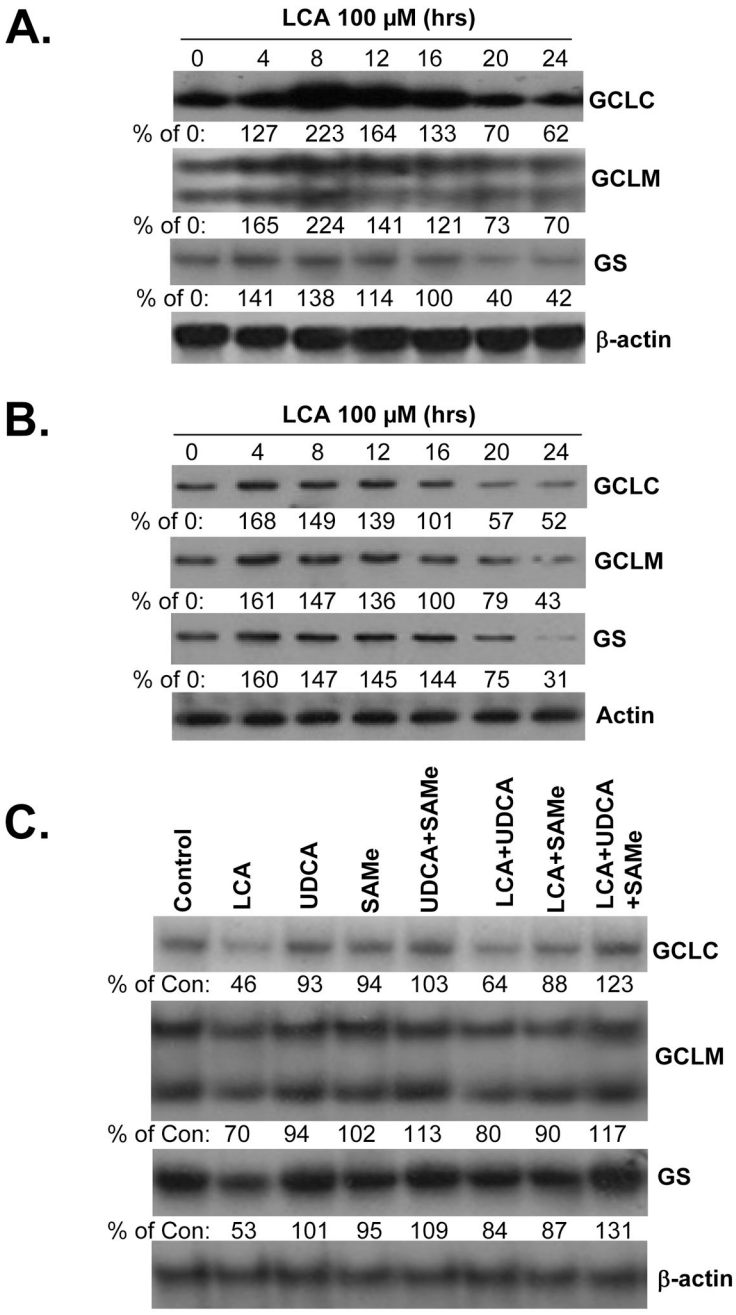

Figure 1.

Effect of LCA treatment in HuH-7 cells on mRNA (part **A**) and protein (part **B**) levels of GCLC, GCLM and GS. RNA and protein were isolated from HuH-7 cells treated with LCA (100 μM) for up to 24 hour for Northern or Western blot analyses (15 μg RNA or protein/lane). Membranes were stripped and re-probed with β-actin for Northern or actin for Western to ensure equal loading. Representative blots from 3 separate experiments are shown and numbers below the blots represent densitometric values expressed as % of 0 time control. Part **C)** Effects of UDCA and SAMe treatment on LCA-mediated lowering of GCLC, GCLM and GS mRNA levels in HuH-7 cells. HuH-7 cells were treated with 100 μM of LCA, UDCA, SAMe, alone or together for 20 hours and RNA was extracted for Northern

blot analyses (15 μg per lane) as described in Methods. Membranes were stripped and re-probed with β-actin to ensure equal loading. Representative blots from 3 experiments are shown and numbers below the blots are densitometric values expressed as % of untreated controls.

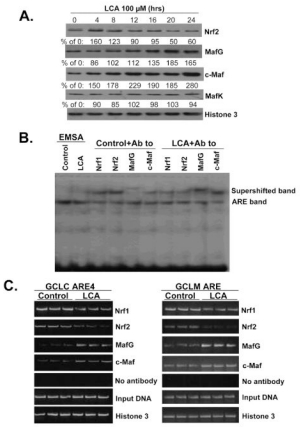

Figure 2.

Effect of LCA treatment in HuH-7 cells on nuclear protein levels of Nrf2 and Mafs and ARE nuclear binding activity by these proteins. Part **A**) Western blot analysis. Nuclear proteins were isolated from HuH-7 cells treated with LCA (100 μM) for up to 24 hours (15 μg protein/lane). Membranes were stripped and re-probed with histone 3 to ensure equal loading. Representative blots from 3 separate experiments are shown and numbers below the blots represent densitometric values expressed as % of 0 time control. Part **B**) EMSA and supershift analysis. HuH-7 cells were treated with LCA (100 μM) or vehicle control for 20 hours and antibodies to Nrf1, Nrf2, MafG and c-Maf were used to compare relative amount of binding of these transcription factors to ARE as described in Methods. Part **C**) ChIP analysis. HuH-7 cells were treated with LCA (100 μM) or vehicle control for 20 hours, then processed for ChIP assay as described in Methods. PCR products from amplification of the ARE sites following immunoprecipitation with antisera against Nrf2, Nrf1, c-Maf, MafG and Histone 3 demonstrate LCA treatment led to decreased Nrf2 and Nrf1 binding to the ARE sites, while c-Maf and MafG binding increased. Input genomic DNA (gDNA input) was used as a positive control and a no antibody immunoprecipitation (no Ab) was used as a negative control.

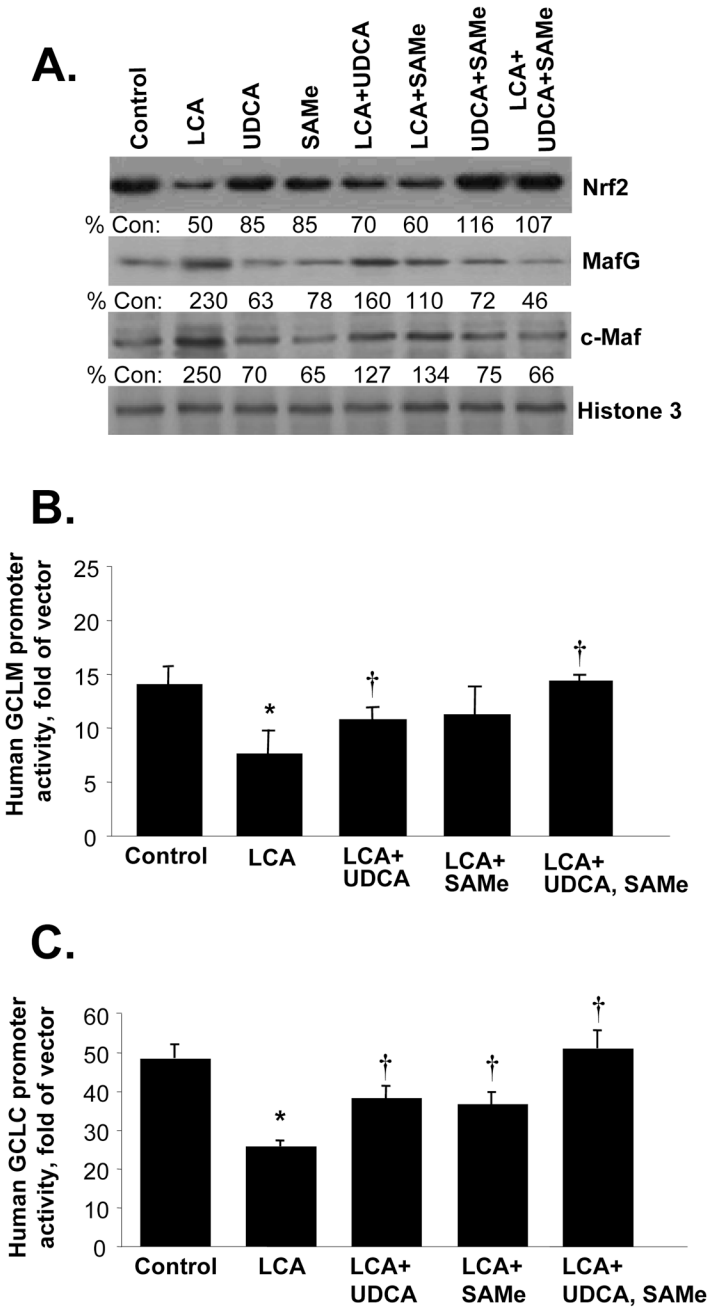

Figure 3.

Effects of LCA, UDCA and SAMe on Nrf2, MafG and c-Maf expression (part **A**) and GCL promoter activities (parts **B** and **C**). For part **A**, HuH-7 cells were treated with 100 μM of LCA, UDCA, SAMe, alone or together for 20 hours and nuclear proteins were extracted for Western blot analysis as described in Methods. Numbers below the blots represent densitometric values expressed as % of control. For promoter activity analysis, HuH-7 cells were transfected with human GCLC or GCLM promoter constructs and treated with the same concentrations of LCA, with or without UDCA and/or SAMe as above for 20 hours. Promoter activity was measured as described in Methods. Results are mean±SE from 3 independent experiments done in triplicates. *$p<0.05$ vs. control, †$p<0.05$ vs. LCA

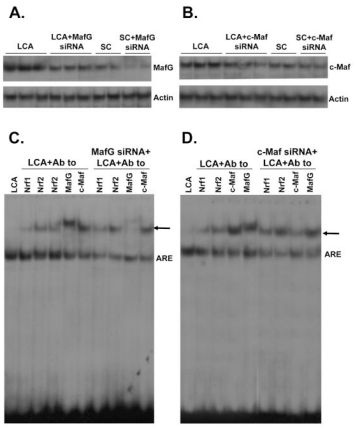

Figure 4.

Effects of MafG and c-Maf siRNA on MafG and c-Maf expression (parts **A** and **B**) and ARE nuclear binding activity (parts **C** and **D**). HuH-7 cells were treated with MafG, c-Maf or scrambled (SC) siRNA for 24 hours at which time LCA was added for another 20 hours. Cells were then processed for Western blot analysis for respective Maf proteins (15 μg/lane) or EMSA with supershift analyses as described in Methods using 15 μg of nuclear protein per lane and antibodies against various proteins as indicated. Arrows point to supershifted bands.

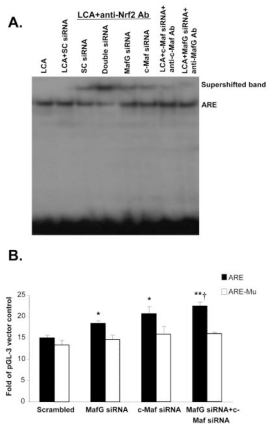

Figure 5.

Effect of MafG, c-Maf or double knockdown on Nrf2 nuclear binding to ARE and ARE-dependent promoter activity. **A)** HuH-7 cells were treated with scrambled (SC), MafG, c-Maf or combined MafG and c-Maf siRNA for 24 hours followed by LCA treatment for another 20 hours. EMSA and supershift analysis was done as described in Methods using antibodies to Nrf2, MafG and c-Maf. **B)** HuH-7 cells were treated with the same siRNAs as above for 24 hours and then transfected with ARE promoter construct containing native or mutated sequences as described in Methods. Results represent mean±SE from 3 independent experiments done in triplicates. *$p<0.05$ vs. scrambled, **$p<0.005$ vs. scrambled, †$p<0.05$ vs. MafG siRNA.

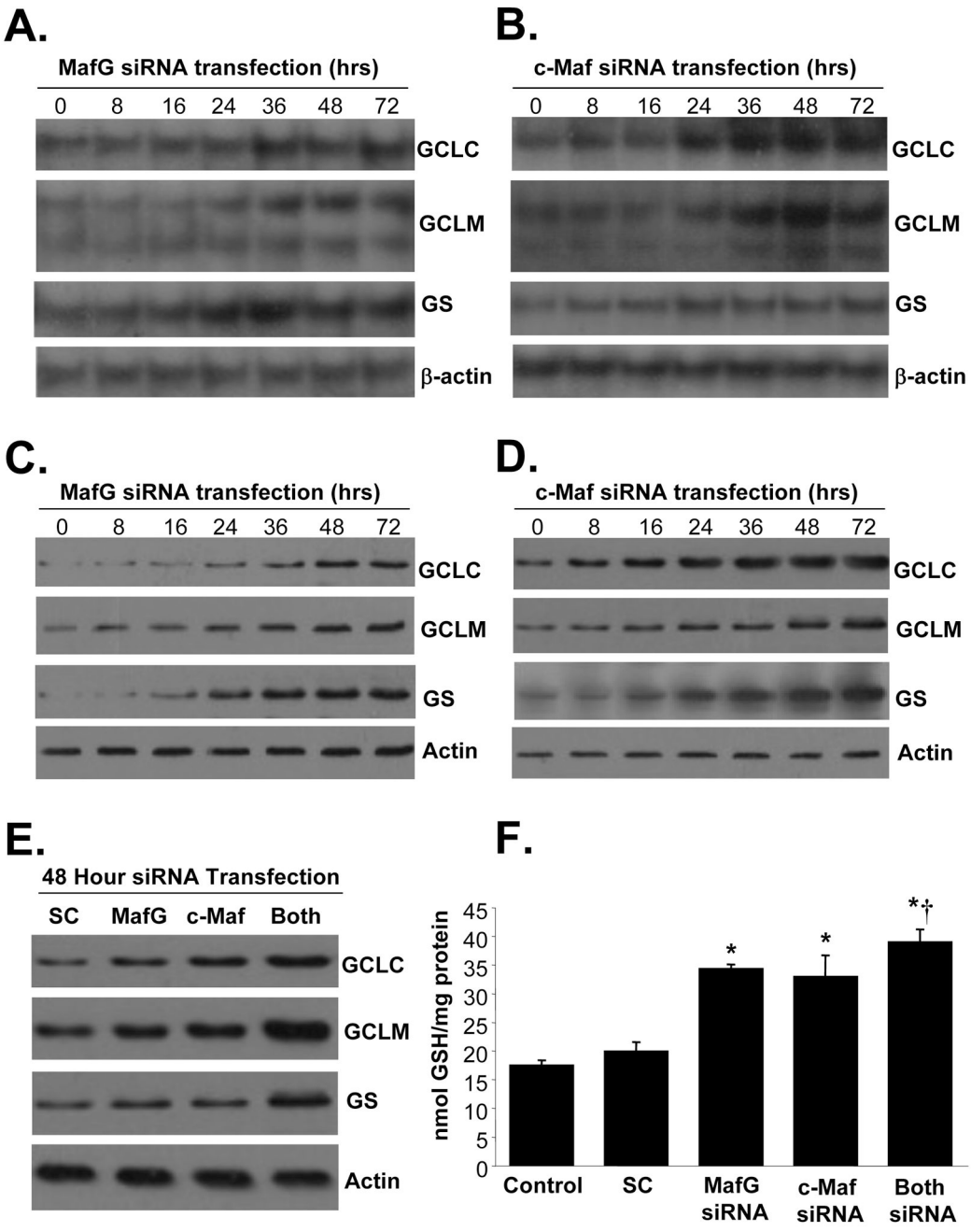

Figure 6.

Effect of MafG, c-Maf or double knockdown on expression of GSH synthetic enzymes and GSH levels. HuH-7 cells were treated with MafG (**A** and **C**) or c-Maf (**B** and **D**) siRNA for up to 72 hours and processed for Northern (**A** and **B**) or Western (**C** and **D**) analyses as described in Methods. In **E**), HuH-7 cells were treated with scrambled (SC), MafG, c-Maf, or both siRNA for 48 hours and processed for Western blot analyses for GCLC, GCLM and GS. In **F**), GSH levels were measured following the same treatments as in **E**. Results are mean±SE from 3 to 4 independent determinations. *p<0.001 vs. SC, †p<0.05 vs. MafG or c-Maf siRNA alone.

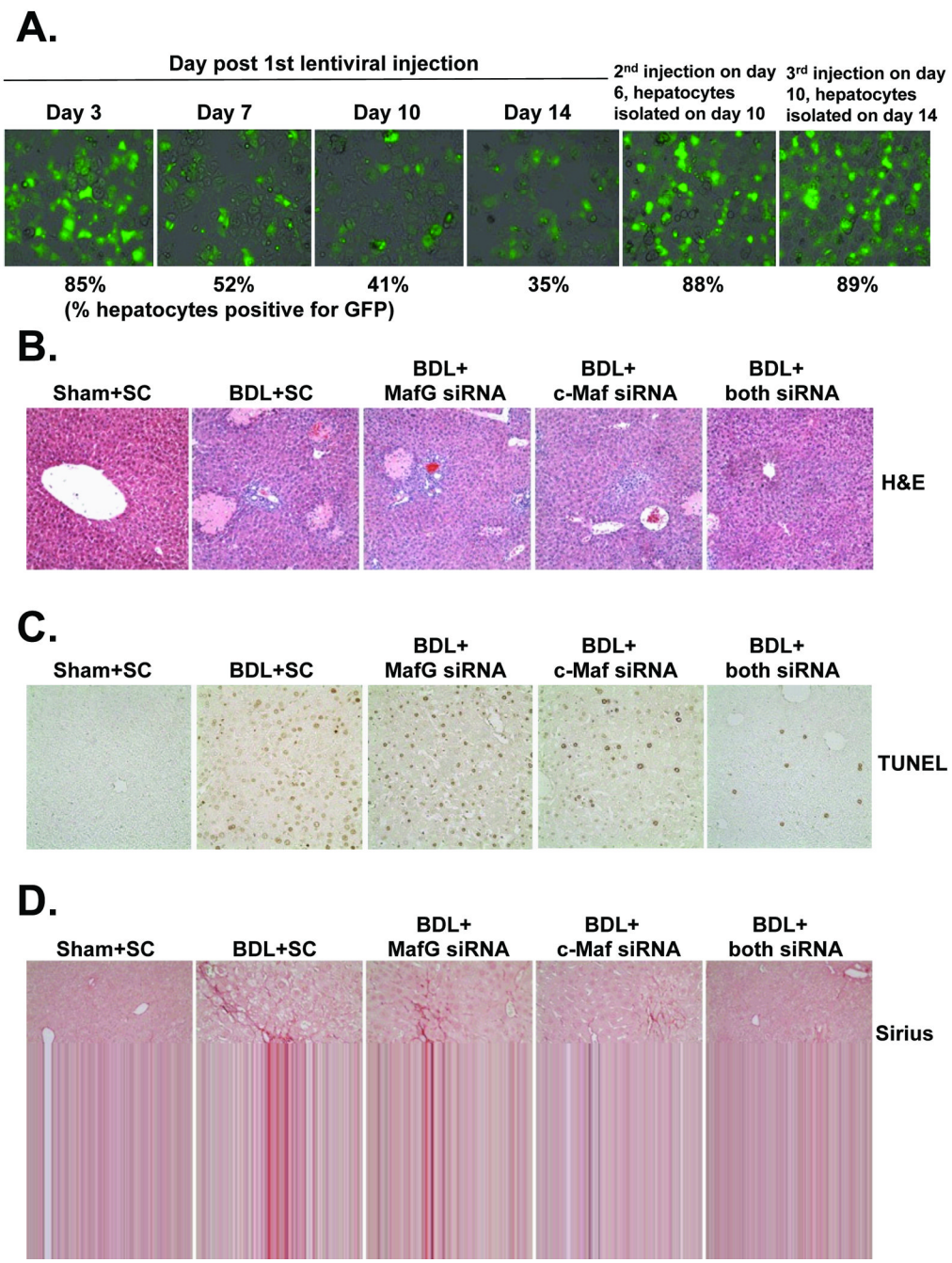

Figure 7.

Effects of in vivo MafG and c-Maf knockdown in BDL mice. Mice were treated with lentivirus carrying scrambled (SC), MafG, c-Maf or both MafG and c-Maf siRNA. In part **A**, pilot experiment showed transduction efficiency as estimated by % hepatocytes that were positive for GFP to fall significantly by day 7 following a single injection. However, transduction efficiency was excellent even at day 14 with repeated injections (day 6 and 10). Mice were subjected to BDL or sham surgery and injected with lentivirus at the time of BDL, on day 6 and 10 and sacrificed on day 14 for determination of necrosis by H&E (**B**), apoptosis by TUNEL (**C**) and fibrosis by Sirius red staining (**D**). See Table I for quantitation of these (100× for **A** and **B** and **C**). See Methods for details.

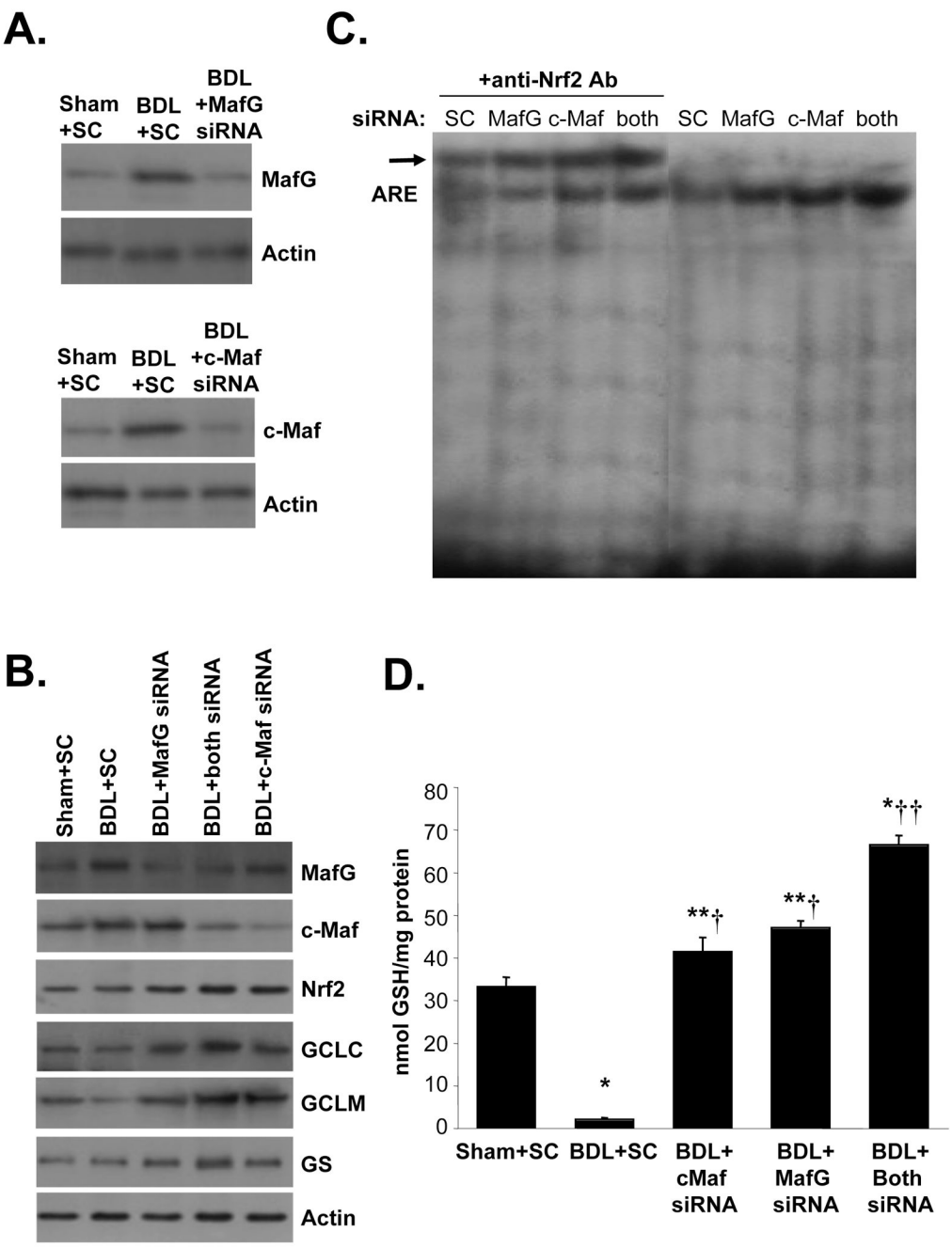

Figure 8.

Effects of in vivo MafG and c-Maf knockdown in BDL mice on gene expression, ARE nuclear binding and GSH levels. Mice were subjected to BDL or sham surgery and treated with lentivirus carrying scrambled (SC), MafG, c-Maf or both MafG and c-Maf siRNAs as described in Methods and sacrificed on day 14. Parts **A** and **B** show Western blot analyses of MafG, c-Maf, Nrf2, GCLC, GCLM and GS. Part **C** shows EMSA and supershift analysis for Nrf2 binding to ARE using nuclear proteins from BDL mice treated with SC, MafG, c-Maf or both siRNAs. Part **D** summarizes hepatic GSH levels in these mice. Results are mean±SE from 3 to 4 mice for each condition. *p<0.001 vs. Sham+SC, **p<0.05 vs. Sham+SC, †p<0.005 vs. BDL+SC, ††p<0.001 vs. BDL+SC and BDL+either Maf siRNA.

Table 1

Effects of c-Maf and MafG siRNA on Liver Injury and Fibrosis 14 Days After BDL

	Sham+ SC	BDL+ SC	BDL+ c-Maf siRNA	BDL+ MafG siRNA	BDL+ both siRNA
Serum or plasma levels:					
ALT (Units/L)	39±4	919±105*	104±26**†	75±13**†	90±16**†
ALP (Units/L)	93±5	643±37*	314±48*†	327±44*†	279±26*†
Bilirubin (μmol/L)	18±4	286±55**	111±39**†	135±25**	78±12••†
Liver Immunohistochemistry:					
Necrosis (% of total)	0.1±0.01	23.6±1.6*	17.4±0.6*†	18.0±0.6*†	13.0±0.6*††
Apoptosis (% of total)	1.2±0.3	18.7±2.6*	14.5±1.8*†	13.9±2.1*†	11.0±1.1*††
Sirius Red (% of total)	0.5±0.1	6.4±0.5*	4.7±0.6*	5.2±0.3*	2.8±0.6*††

Results are mean±SEM from 4 to 8 mice for each group. Mice were treated with c-Maf, MafG and scrambled (SC) siRNAs and BDL or sham surgery as described in Methods.

* p<0.01 vs. sham+SC,

** p<0.05 vs. sham+SC,

† p<0.05 vs. BDL+SC,

†† p<0.05 vs. BDL+SC and BDL+either Maf siRNA alone